



Published in final edited form as:

*Am J Physiol Regul Integr Comp Physiol.* 2017 April 01; 312(4): R585–R596. doi:10.1152/ajpregu.00481.2016.

## Upregulation of fatty acid amide hydrolase in the dorsal periaqueductal gray is associated with neuropathic pain and reduced heart rate in rats

Caron Dean<sup>1,3</sup>, Cecilia J. Hillard<sup>2</sup>, Jeanne L. Seagard<sup>1,3</sup>, Francis A. Hopp<sup>3</sup>, Quinn H. Hogan<sup>1,3</sup>

<sup>1</sup>Department of Anesthesiology, Medical College of Wisconsin, Milwaukee, Wisconsin

<sup>2</sup>Department of Pharmacology, Medical College of Wisconsin, Milwaukee, Wisconsin

<sup>3</sup>Zablocki Veterans Affairs Medical Center, Milwaukee, Wisconsin

### Abstract

Nerve damage can induce a heightened pain response to noxious stimulation, which is termed hyperalgesia. Pain itself acts as a stressor, initiating autonomic and sensory effects through the dorsal periaqueductal gray (dPAG) to induce both sympathoexcitation and analgesia, which prior studies have shown to be affected by endocannabinoid signaling. The present study addressed the hypothesis that neuropathic pain disrupts autonomic and analgesic regulation by endocannabinoid signaling in the dPAG. Endocannabinoid contents, transcript levels of endocannabinoid signaling components, and catabolic enzyme activity were analyzed in the dPAG of rats at 21 days after painful nerve injury. The responses to two nerve injury models were similar, with two-thirds of animals developing hyperalgesia that was maintained throughout the postinjury period, whereas no sustained change in sensory function was observed in the remaining rats. Anandamide content was lower in the dPAG of rats that developed sustained hyperalgesia, and activity of the catabolic enzyme fatty acid amide hydrolase (FAAH) was higher. Intensity of hyperalgesia was correlated to transcript levels of FAAH and negatively correlated to heart rate and sympathovagal balance. These data suggest that maladaptive endocannabinoid signaling in the dPAG after nerve injury could contribute to chronic neuropathic pain and associated autonomic dysregulation. This study demonstrates that reduced anandamide content and upregulation of FAAH in the dPAG are associated with hyperalgesia and reduced heart rate sustained weeks after nerve injury. These data provide support for the evaluation of FAAH inhibitors for the treatment of chronic neuropathic pain.

### Graphical Abstract

---

Address for reprint requests and other correspondence: C. Dean, Dept. of Anesthesiology, Research Service 151, Zablocki VA Medical Center, Milwaukee, WI 53295 (cdean@mcw.edu).

#### AUTHOR CONTRIBUTIONS

C.D., J.L.S., C.J.H., and Q.H.H. conception and design of research; C.D. and J.L.S. performed experiments; C.D. and C.J.H. performed the tissue analyses; C.D., J.L.S., C.J.H. and F.A.H. analyzed and interpreted data; C.D., F.A.H., and Q.H.H. prepared figures; C.D. drafted manuscript; J.L.S., C.J.H., F.A.H. and Q.H.H. edited and revised manuscript; C.D., J.L.S., C.J.H., F.A.H., and Q.H.H. approved final version of manuscript.

#### DISCLOSURES

No conflicts of interest, financial or otherwise, are declared by the author(s).



### Keywords

endocannabinoids; autonomic; stress response; neuropathic pain; hyperalgesia; FAAH

NEUROPATHIC PAIN is a critical treatment challenge that accompanies many injury and disease states in which peripheral nerves are damaged. Sensory abnormalities include hyperalgesia, in which pain from noxious stimuli has increased intensity. Current treatments are inadequate and a better understanding of the pathophysiology of sensory pathways that lead to the development of neuropathic pain is necessary to improve management. There is substantial evidence for cannabinoid modulation of neuropathic pain at both central and peripheral sites (23). Providing the anatomic framework for cannabinoid signaling, G protein-coupled cannabinoid 1 (CB1) receptors are located throughout the central nervous system and peripherally in postganglionic nerve terminals, whereas CB2 receptors are predominant in immune cells (21). The endogenous ligands (i.e., endocannabinoids) include *N*-arachidylethanolamine (anandamide or AEA) and 2-arachidonoylglycerol (2-AG). The synaptic concentrations of these ligands are tightly regulated by their catabolic enzymes, which include fatty acid amide hydrolase (FAAH) and monoacylglycerol lipase (MAGL), which hydrolyze AEA and 2-AG, respectively (3, 8).

There is evidence to suggest that altered endocannabinoid signaling in the periphery and spinal cord facilitates analgesia after nerve injury. Cannabinoid receptors are found in somatosensory processing components, including the dorsal root ganglia (DRG), primary afferent neurons, and dorsal horn (18, 29, 60). An increase in CB1 receptors and

endocannabinoids in the ipsilateral DRG and the spinal cord follow injury, which suggests a site of action for systemically administered cannabinoids in the attenuation of hyperalgesia in models of neuropathic pain (4, 20, 38, 47). Cannabinoids also suppress evoked responses in C-fiber nociceptors and in wide dynamic range dorsal horn neurons (16, 29, 33). However, systemic administration of CB1 receptor agonists could additionally activate supraspinal cannabinoid signaling in the amygdala, thalamus, periaqueductal gray (PAG), and rostroventromedial medulla, for example (37, 41–44). Early studies of PAG-evoked analgesia established that it was site-specific, with opioid-dependent actions identified in the ventral region and opioid-independent and endocannabinoid-dependent mechanisms in the dorsal PAG (dPAG) (7, 42, 63). Increased dPAG endocannabinoid concentrations are associated with analgesic effects in neuropathy and subcutaneous formalin models (51, 59), which supports the hypothesis that the dPAG is a site of central antihyperalgesic responses to cannabinoid agonists (20, 52).

It is well established that the somatic sensory system and cardiovascular function are closely linked, as acute noxious stimuli increase sympathetic nerve activity and blood pressure, activating a feedback loop by which increased blood pressure elevates pain thresholds (5, 49, 55). The dPAG has been identified as a site supporting such sympathosensory integration where maladaptive changes that could contribute to chronic pain conditions would also be likely to evoke autonomic and circulatory disturbances (5, 39, 46). There is very little information available on the autonomic and cardiovascular consequences of neuropathic pain in animals or humans. One study of chronic constriction injury of the sciatic nerve in rats demonstrates an initial elevation in blood pressure and heart rate that transitions to normotension and bradycardia supported by increased parasympathetic tone, as neuropathic pain develops (31). These data translate in part to human subjects, in whom either sympathoinhibition, bradycardia, and depressor effects or sympathoexcitation, tachycardia, and increased blood pressure accompanied chronic muscle pain, yet the response type could not be predicted by the pain rating (19). Although it is clear that autonomic and sensory interactions are important in pain states, the definitive changes and the underlying mechanisms are not known (5). The first aim of this study was to assess whether the autonomic and cardiovascular changes associated with development of neuropathic pain are consistent with disruption of normal cardiovascular-sensory interactions. There is evidence that, in addition to its antinociceptive actions, the endocannabinoid system in the dPAG influences autonomic function, as microinjection of anandamide elicits an increase in sympathetic nerve activity and alters cardiovascular parameters (10, 13). Furthermore, both antinociceptive and autonomic effects associated with stress are attenuated by CB1 receptor blockade in the dPAG (10, 28, 42). Together, these observations suggest that endocannabinoid signaling in the dPAG could contribute to sympatho-sensory integration. Therefore, the second aim of this study was to test our hypothesis that dysregulation of endocannabinoid signaling in the dPAG underlies shifts in both autonomic and analgesic functions during neuropathic pain.

## METHODS

The protocols for the study were approved by the Animal Care and Use Committees at the Medical College of Wisconsin and the Zablocki Department of Veterans Affairs Medical

Center. Male Sprague-Dawley rats (320–330 g,  $n = 54$  total) were obtained from Charles River (Wilmington MA) and were maintained and used according to the National Institutes of Health *Guide for the Care and Use of Laboratory Animals* and in compliance with federal, state, and local laws. Animals were housed individually, for radiotelemetric blood pressure monitoring, in a room maintained at  $22 \pm 1^\circ\text{C}$  at 35–45% humidity. Animals had free access to food (Purina laboratory rodent diet 5001) and water, and bedding was Beta Chip (Warrensburg, NY).

### **Instrumentation and blood pressure monitoring.**

Animals were implanted with a PA-C10 transmitter [Data Sciences International (DSI), St. Paul, MN] to monitor arterial blood pressure. Rats were anesthetized with isoflurane (5% induction, 1.75–2% maintenance) in  $\text{O}_2$ , and the cannula (0.43-mm OD polyethylene) attached to the transmitter was inserted into the left femoral artery through a small inguinal incision, with care taken to avoid manipulation of the adjacent femoral nerve. The transmitter was fixed in a subcutaneous pocket on the left flank of the rat, and the incision was closed with 3–0 silk suture. A redundant loop in the cannula allowed for the growth of the rat. Animals were treated with carprofen (5 mg/kg sc) at the start of surgery and on *day 1* postimplantation. After 7 days, animals were anesthetized again for removal of inguinal stitches and for either spared nerve injury, modified spinal nerve ligation surgery, or sham surgery (details below). Animals were treated with carprofen (5 mg/kg sc) at the start of surgery. No postoperative analgesia was administered to avoid confounding effects on development of pain phenotype post injury. Blood pressure was monitored 2 days before, and on the day of, nerve injury/sham surgery, and on *days 1, 3, 7, 10, 14, and 21* postinjury/postsham surgery. Recording was performed from 7 to 9 AM, during times of minimal movement to avoid the elevated pressure that accompanies activity, and before behavioral evaluation of hyperalgesia (see below) to avoid confounding effects of sensory testing.

### **Heart rate variability determination.**

Resting blood pressure was analyzed for heart rate and heart rate variability (HRV) to indicate autonomic changes to the heart, using the DSI Dataquest A.R.T. software system. Power spectral analysis of heart rate was used to determine HRV from blood pressure data as described previously (22). A cubic algorithm was used to interpolate blood pressure data sampled at 500 Hz to 2 kHz. The blood pressure data were used to calculate an interbeat interval (IBI) series from three 5-min segments, each with 5 overlapping (50%) subsegments of 512 points. The IBI was converted into an instantaneous heart rate using the formula: heart rate (beats/min) =  $60/\text{IBI}$  (s). The IBI values were then interpolated at 50 Hz (cubic algorithm), detrended, and the mean was suppressed to create the data points equally spaced in time for further analysis. Utilizing a Hanning window, the power was calculated for each data set over the frequency ranges of 0.25–1 Hz (low frequency, LF) and 1–3 Hz (high frequency, HF), with the results from the three segments averaged for the final determination of density within each frequency band. LF and HF powers were normalized and expressed as percentages of total power (LF + HF powers), and the LF/HF ratio was calculated from these values. Although HF power is generally accepted as a reflection of vagal modulation of heart rate, the LF power/HF power ratio is thought to represent sympathovagal balance (15, 40). Although the use of this parameter is controversial, it remains widely used in both research

and clinical applications as a noninvasive indicator of the relative activity of cardiac sympathetic and parasympathetic innervation that may be more accurate for short-term recordings as used in this study (2, 45). An increase in the LF power/HF power ratio indicates a change to a relatively higher sympathetic vs. vagal cardiac modulation, whereas a decrease reflects the opposite. This is supported by data that clearly demonstrate a direct correlation between baseline heart rate and LF/HF power ratio (13).

### **Spared nerve injury (SNI).**

An incision was made through the skin and the biceps femoris muscle on the lateral surface of the right thigh to expose the sciatic nerve and its three terminal branches (tibial, common peroneal, and sural nerves). The tibial and common peroneal nerves were ligated with 6–0 silk suture and transected, while care was taken to avoid trauma to the sural nerve, which remained intact. The muscle layers were closed with 5–0 absorbable polyglycolic suture and the skin layer was closed with staples. Sham spared nerve injury surgery was performed on control animals, in which all three terminal nerves were exposed but left intact. Staples were removed after 7 days.

### **Enhanced spinal nerve ligation (eSNL).**

To more broadly examine the effect of neuropathy on dPAG function, we employed a second established rat model of neuropathic pain (14, 36). The right lumbar paravertebral region was exposed through a posterior midline incision, and subperiosteal removal of the sixth lumbar transverse process was performed. The fifth lumbar spinal nerve was tightly ligated with 6–0 silk suture and transected distal to the ligature. A loose loop of chromic gut suture (4–0; Ethicon, Somerville NJ) was placed around the ipsilateral fourth lumbar spinal nerve, leaving at least 1 mm of space from the nerve circumferentially. The muscle incision was closed with 4–0 resorbable polyglactin suture, and the skin layer was closed with staples. Sham eSNL surgery was performed on control animals, in which the fifth spinal nerve was exposed but left intact. Staples were removed after 7 days.

### **Behavioral evaluation of hyperalgesia.**

Neuropathic pain is typified by hyperalgesia behavior, which is an enhanced response to a noxious stimulus. Animals were evaluated for hyperalgesia responses after each resting blood pressure monitoring period. Animals were placed individually in clear plastic enclosures on an elevated one-fourth-in. wire grid for behavioral evaluation of hyperalgesia. After an acclimation period that allowed animals to cease exploratory activity, the point of a 22-gauge spinal anesthesia needle was applied to the lateral part of the plantar surface of the paw for SNI animals, or to the center region of the hindpaw for eSNL animals. Needle force was sufficient to indent, but not penetrate, the skin. The behaviors induced by this stimulus were of two types, either a brisk, simple withdrawal with immediate return of the foot to the wire floor, which is typical of normal animals, or a hyperalgesia-type response that consisted of sustained elevation of the paw with shaking, licking, and grooming (22, 27). This hyperalgesia response has been specifically correlated with conditioned avoidance in nerve-injured rats indicating its aversiveness (63). In contrast, simple responses to calibrated monofilaments (von Frey test), such as are used for determination of the threshold for withdrawal from mechanical stimulation, are not associated with aversiveness (63). We

therefore used the frequency of hyperalgesia-type responses during needle testing as the most meaningful measure of pain for stratifying animals. Specifically, the response type was noted for each of 5 applications, separated by at least 10 s, to each hindpaw, and repeated after 2 min, for a total of 10 touches to each paw. The number of hyperalgesia-type responses was normalized to a percent response (hyperalgesia response rate). Peripheral nerve injury results in a high interindividual variance of hyperalgesia response rates (27), and rats that demonstrated a hyperalgesia response rate >20% on *day 21* were defined hyperalgesic and assigned to the Hyperalgesia group, whereas those responding <20% were assigned to the Non-Hyperalgesia group (22).

### Tissue collection.

On *day 21*, after the blood pressure monitoring and the hyperalgesia behavior testing period, animals were deeply anesthetized with isoflurane (5%) in O<sub>2</sub> and decapitated. The brain was removed and the midbrain tissue along the full length of the cerebral aqueduct was quickly excised. Under a microscope, the dPAG was dissected at the lateral and dorsal borders of the periaqueductal gray matter, and a ventral cut was made at the midcerebral aqueduct. Although there are no anatomic distinctions of PAG columns, this approach ensures that the dissected tissue sample is limited to the dPAG, which includes the dorsal, dorsomedial, and dorsolateral columns. Tissue samples were frozen in liquid nitrogen and stored at -80°C for subsequent analysis. Endocannabinoid content, expression of mRNA for components of the endocannabinoid signaling system, or FAAH activity analyses were performed on dPAG samples from SNI rats. Samples from eSNL rats were analyzed for expression of FAAH mRNA and provided data similar to that for SNI rats. Therefore, to reduce animal use, lipid measurements and enzyme activity assays were not performed on samples from eSNL rats.

### Lipid measurement.

To analyze the dPAG content of the *N*-acylethanolamines (NAEs) anandamide, *N*-oleoylethanolamine (OEA), and *N*-palmitoylethanolamine (PEA), and the *O*-acylglycerols 2-AG, and 2-oleoyl[<sup>3</sup>H]glycerol (2-OG), tissue samples were subjected to a lipid extraction process as described previously (50). Briefly, tissue samples were weighed and homogenized in acetonitrile containing 34 pmol of [<sup>2</sup>H<sub>8</sub>]AEA and 66 pmol of 2-[<sup>2</sup>H<sub>8</sub>]AG for extraction. Tissue was homogenized, sonicated for 30 min, and incubated overnight at -10°C to precipitate the proteins. Particulates were removed from acetonitrile by centrifugation at 1,500 rpm, the supernatants were removed and evaporated to dryness under N<sub>2</sub> gas, and the extracted lipids were resuspended in 30 µl of mobile phase (85% methanol, 15% ddH<sub>2</sub>O with 5 µl acetic acid and 0.0075 g ammonium acetate per 100 ml) for liquid chromatography/mass spectrometry/mass spectrometry (LC/MS/MS) analysis.

The LC/MS/MS analysis was conducted on 5 µl of sample using an Agilent Technologies 6460 Triple Quad LC/MS. Samples were separated using a reverse-phase C<sub>18</sub> column (Kromasil, 250 × 2 mm, 5 µm diameter) beginning in 15% mobile *phase A* (100% ddH<sub>2</sub>O with 5 µl acetic acid and 0.0075 g ammonium acetate per 100 ml) and 85% mobile *phase B* (100% methanol with 5 µl acetic acid and 0.0075 g ammonium acetate per 100 ml) and ramping to 100% *B* over 8 min; remaining at 100% *B* until 23 min, then returning to 85% mobile *phase B*. Selective ion monitoring, made in the positive ion mode, was used to detect

the daughter ions of [<sup>2</sup>H<sub>8</sub>]AEA (*m/z* 62), AEA (*m/z* 62), OEA (*m/z* 62), PEA (*m/z* 62), 2-[<sup>2</sup>H<sub>8</sub>]AG and 1,3-AG (*m/z* 293.1), 2-AG and 1,3-AG (*m/z* 287.1) and 2-OG and 1,3-OG (*m/z* 286.1). 2-AG and 1,3-AG were combined, as were 2-OG and 1,3-OG. Lipid contents were normalized to tissue wet weight.

### Real time RT-PCR.

Expression levels of mRNA were measured for FAAH, MAGL, and CB1 receptors in the dPAG, using standard techniques. Total RNA was extracted from each dPAG sample using RNeasy Mini Kit (Qiagen, Valencia, CA). cDNA was synthesized using iScript reverse transcriptase (Bio-Rad, Hercules, CA). mRNA was quantified using SYBR-Green as the detection agent and amplifications were performed with the Eppendorf Mastercycler Realplex in 25 µl reaction volumes containing cDNA, primers, and iQ Supermix (Bio-Rad). Thermal cycling proceeded with one amplification cycle of denaturation at 95°C for 2 min, followed by 45 cycles of 95°C for 15 s, 55°C for 15 s, and 68°C for 20 s. The cycle at which amplification reached threshold (*C<sub>T</sub>*) was determined for each amplicon. All reactions were performed in duplicate. Results were calculated by subtracting *C<sub>T</sub>* of hypoxanthine guanine phosphoribosyltransferase (HPRT) as a baseline control (*C<sub>T</sub>*) and normalized to 200<sup>-*C<sub>T</sub>*</sup>. Specificity of the RT-PCR reaction was confirmed by melting curves. Efficiencies were 0.9–1.1 for each amplicon.

The following sequence-specific primers were used, listed as 5' to 3': HPRT forward GCA GAC TTT GCT TTC CTT GG and reverse CCG CTG TCT TTT AGG CTT TG; FAAH forward GAG GCT GGC TTT CAA CTC AC and reverse TTC GGA AGA CAG GCC AAT AC; MAGL forward CAC CTC TGA TCC TTG CCA AT and reverse GAT GAG TGG GTC GGA GTT GT; CB1R forward TCA GCA AGA AGT CAT CAG TAA GAG and reverse CCA CCA TCC TCC ACA CTC C.

### FAAH activity assay.

Frozen dPAG tissue samples were weighed and homogenized in 10 vol TME buffer (50 mM Tris-HCl, pH 7.4; 3 mM MgCl<sub>2</sub> and 1 mM EDTA). Homogenates were centrifuged at 12,000 rpm for 20 min at 4°C, and the pellet containing a crude membrane fraction was resuspended in 10 vol TME buffer for FAAH activity assay. Samples were frozen at -80°C until assayed. Protein concentrations were determined by the Bradford method (Bio-Rad).

FAAH activity was measured as the conversion of anandamide labeled with <sup>3</sup>H in the ethanolamine portion of the molecule ([<sup>3</sup>H]AEA; 60 Ci/mmol; American Radiolabeled Chemicals, St. Louis, MO), [<sup>3</sup>H]AEA to [<sup>3</sup>H]ethanolamine, as reported previously (13). Membranes from each sample (0.9 mg protein) were incubated in TME buffer (0.5 ml) containing 1.0 mg/ml fatty acid-free BSA and 0.2 nM [<sup>3</sup>H]AEA. Non-FAAH-mediated hydrolysis was determined by a duplicate incubation carried out in the presence of the FAAH inhibitor URB597 (cyclohexylcarbamic acid 3'-carbamoylbiphenyl-3-yl ester; 1 µM) (Tocris Bioscience, Minneapolis MN) that was subtracted from the total hydrolysis. After hydrolysis for 10 min at 30°C, the incubations were stopped with the addition of 2 ml chloroform/methanol (1:2), and after standing on ice for 30 min with regular vortexing, 0.67 ml chloroform and 0.6 ml water were added. Aqueous and organic phases were separated by

centrifugation at 2,500 rpm for 5 min. The amount of  $^3\text{H}$  in 500  $\mu\text{l}$  of the aqueous phase was determined by liquid scintillation counting, and the conversion of [ $^3\text{H}$ ]AEA to [ $^3\text{H}$ ]ethanolamine was calculated and normalized to amount of membrane protein.

### Statistical analysis.

Blood pressure, heart rate, HRV, and hyperalgesia response rate were calculated for each monitoring period on *days 1, 3, 7, 10, 14, and 21* postinjury. Baseline (prenerve injury, *day -1*) levels were calculated by averaging values for the 2 days before, and the day of but before, nerve injury. Heart rate, HF power, LF power/HF power ratio, mean arterial blood pressure, and hyperalgesia response rate were plotted against time and compared for group and time points using one-way ANOVA and multiple-comparison Holm-Sidak post hoc tests.

Correlational analyses were performed for hyperalgesia response rate, heart rate, and HRV parameters on *day 21* against transcript levels of FAAH for dPAG tissue samples from *day 21* postinjury. The change in heart rate and HRV parameters were also plotted against hyperalgesia response rate at 21 days after injury. Linear regression analyses were performed in SigmaPlot 11 to evaluate potential associations. Significance was set at  $P < 0.05$  for  $r^2$  values produced by linear regression analysis.

Transcript levels of FAAH, FAAH enzyme activity and endocannabinoid content in the dPAG at 21 days after SNI were compared for Non-Hyperalgesia versus Hyperalgesia groups with unpaired *t*-tests with the level of significance set at the 0.05 level.

## RESULTS

### Hyperalgesia after nerve injury.

Hyperalgesia response rates ranged from 0 to 90% at 21 days postnerve injury (Fig. 1). Animals were grouped according to their hyperalgesia response rates to noxious mechanical stimulation of the hindpaw 21 days after nerve injury. Of 23 SNI rats, 14 had a response rate  $>20\%$  and so were assigned to the Hyperalgesia group (group mean of 66%), whereas 9 rats demonstrated a response rate  $<20\%$  and were assigned to the Non-Hyperalgesia group (group mean of 10%) (Fig. 1A). Of 17 eSNL rats, 10 were classified as Hyperalgesia (mean response rate 67%) and 7 grouped as Non-Hyperalgesia (mean response rate 10%) (Fig. 1B). The time course for development of hyperalgesia after SNI (Fig. 2A) and eSNL (Fig. 3) were strikingly similar. Animals displayed no hyperalgesia response to stimulation at baseline before nerve injury, and Sham control animals demonstrated minimal hyperalgesia responses to stimulation over the 21-day study period. After nerve injury, hyperalgesia responses increased in all SNI rats up to *day 3*, but by *day 7* there was a divergence in response, with the response rates of the Hyperalgesia group increasing through *day 21* whereas the response rate of the Non-Hyperalgesia group decreased to baseline and Sham SNI levels. Although the point of divergence occurred by *day 3* in the eSNL rats, hyperalgesia behavior developed similarly to the SNI rats.



### Heart rate and heart rate variability after nerve injury.

Baseline values for LF/HF power ratio (reflecting sympathovagal balance) and HF power (indicating vagal parasympathetic tone) were similar for Hyperalgesia, Non-Hyperalgesia, and Sham nerve injury groups (Figs. 2B and 3B). The LF/HF power ratio of the Hyperalgesia groups gradually decreased over 21 days post-SNI or eSNL, whereas that for the Non-Hyperalgesia groups remained the same as the Sham control groups (Figs. 2B and 3B). At 21 days, there was a significantly lower LF/HF power ratio of the Hyperalgesia groups compared with their Non-Hyperalgesia and Sham control groups (Figs. 2B and 4, A and B). For HF power, the trend was reversed, with an increase in the Hyperalgesia group compared with the Non-Hyperalgesia and Sham control groups at 21 days after injury that reached significance in the SNI rats (Figs. 2C, 3C, and 4, A and B).

The heart rate of the Non-Hyperalgesia and Sham injury groups did not change following injury but heart rate of the Hyperalgesia groups decreased significantly over time post injury (Figs. 2D and 3D). When compared with baseline, the SNI Hyperalgesia group demonstrated a significant drop in heart rate at all time points from *day 3*, leading to a 64.5 beats/min ( $\pm 6.7$  beats/min) fall in heart rate on *day 21* compared with 18.0 ( $\pm 6.6$  beats/min) for the Non-Hyperalgesia group (Figs. 2D and 4A). For eSNL, the heart rate of the Hyperalgesia group fell 53.5 beats/min ( $\pm 6.7$  beats/min) compared with 5.4 ( $\pm 6.7$  beats/min) in the Non-Hyperalgesia rats (Figs. 3D and 4B).

The hyperalgesia response rate demonstrated a negative correlation with the change in heart rate and the change in LF/HF power ratio for both SNI and eSNL rats and was positively correlated to the change in HF power for SNI rats (Table 1). For both SNI and eSNL, baseline blood pressures were similar for all three treatment groups, with pressure increasing slightly but not significantly over the 21 days postinjury (Fig. 4, A and B).

### Lipid content in dPAG after SNI.

In a separate set of animals, SNI rats were assigned to Hyperalgesia (mean response rate  $58.6 \pm 8.9\%$ ) and Non-Hyperalgesia (mean response rate  $14 \pm 4.0\%$ ) groups on *day 21* after injury as described above. Analysis of dPAG tissue demonstrated that anandamide content in the Hyperalgesia group was significantly lower than that in the Non-Hyperalgesia group ( $84.8 \pm 3.9$  vs.  $108.7 \pm 7.0$  fmol/mg tissue) (Fig. 5A). Whereas the OEA and PEA contents in the dPAG were reduced in Hyperalgesia compared with Non-Hyperalgesia rats (OEA  $295.1 \pm 30.3$  vs.  $363.1 \pm 46.7$  fmol/mg; PEA,  $421.3 \pm 48.8$  vs.  $501.7 \pm 64.0$  fmol/mg), the differences were not significant. There were no differences in dPAG content of 2-AG or 2-OG in the Hyperalgesia group compared with Non-Hyperalgesia (2-AG,  $142.1 \pm 5.0$  vs.  $143.61 \pm 11.1$  pmol/mg; 2-OG,  $42.1 \pm 5.6$  vs.  $40.3 \pm 3.0$  pmol/mg) groups.

### Expression of FAAH mRNA in dPAG after nerve injury.

As anandamide concentrations are tightly and negatively regulated by FAAH, we examined expression of FAAH mRNA in the dPAG in separate groups of rats 21 days after SNI and eSNL. The hyperalgesia response rate at 21 days post-SNI showed a strong direct correlation to FAAH mRNA expression in the dPAG ( $r^2 = 0.456$ ;  $P = 0.003$ ) (Fig. 6A) that was higher on average in the Hyperalgesia group compared with the Non-Hyperalgesia group (Fig. 5B).

These data suggest that reduced degradation of anandamide in the dPAG of the Non-Hyperalgesia group can result in reduced pain perception. The change in the LF/HF power ratio was also associated with mRNA expression of FAAH at 21 days after injury while the HF power demonstrated a positive correlation (Table 1). These data suggest that increased hydrolysis of anandamide at 21 days after nerve injury is associated with decreased heart rate and increased parasympathetic tone. There was no correlation between transcript levels of MAGL ( $r^2 = 0.155$ ) or the CB1 receptor ( $r^2 = 0.111$ ) in the dPAG and hyperalgesia responses (Fig. 6, C and D).

The hyperalgesia response rate at 21 days post-eSNL showed a direct correlation to mRNA expression of FAAH in the dPAG ( $r^2 = 0.262$ ;  $P = 0.05$ ) (Fig. 6B). The hyperalgesia response rate demonstrated a negative correlation with both the change in heart rate and the change in LF/HF power (Table 1). The changes in the LF/HF power ratio and heart rate were negatively associated with mRNA expression of FAAH at 21 days (Table 1). Taken together, these data suggest that upregulation of FAAH at 21 days after eSNL is associated with enhanced hyperalgesia behavior and decreased heart rate.

#### FAAH enzyme activity in dPAG after SNI.

FAAH enzyme activity in the dPAG was analyzed in a separate group of SNI rats, assigned to Hyperalgesia (mean response rate  $63.3 \pm 9.2\%$ ) and Non-Hyperalgesia (mean response rate  $4 \pm 2.5\%$ ) groups on *day 21* after injury. In accordance with the FAAH transcript data, the Hyperalgesia group had higher FAAH activity ( $5.08 \pm 0.45$  fmol ethanolamine formed $\cdot\text{min}^{-1}\cdot\text{mg protein}^{-1}$ ;  $n = 5$ ) than the Non-Hyperalgesia group ( $2.25 \pm 0.47$  fmol ethanolamine formed $\cdot\text{min}^{-1}\cdot\text{mg protein}^{-1}$ ,  $n = 6$ ) (Fig. 5C). The FAAH activity level in the Non-Hyperalgesia group is similar to the mean baseline level obtained from uninjured rats ( $1.9 \pm 0.45$  fmol ethanolamine formed $\cdot\text{min}^{-1}\cdot\text{mg protein}^{-1}$ ) (13). These data suggest that, after injury, increased FAAH expression is accompanied by increased FAAH activity in the dPAG of animals that develop hyperalgesia behavior.

## DISCUSSION

We have examined the development of hyperalgesia behavior and autonomic changes in two models of peripheral nerve injury, which showed strongly convergent findings. Animals developed hyperalgesia responses to noxious stimulation of the affected paw in the days immediately following injury, and two-thirds of rats maintained hyperalgesia behavior for 3 wk after nerve injury, which compares to the prevalence of chronic pain after physical trauma in humans (58). In addition, there was a distinct variability in the magnitude of sensory responses to each stereotyped nerve injury, as is found in humans. The presence, absence, and variation of hyperalgesia behavior after a peripheral nerve injury is recognized (27), yet remains unexplained. Variability in the anatomy of peripheral nerve distribution (54) or physical tissue damage at the injury site or surgical technique (14) could contribute to the individual variation, but genetic or environmental factors may also predispose an animal to develop pain behavior after injury (48, 56).

Hyperalgesia, maintained for 21 days after nerve injury, was associated with a significant drop in sympathovagal balance and heart rate. Sympathosensory integration is a major

component of the response to stress that is coordinated in the central stress network that includes cortical structures, amygdala, hypothalamus, midbrain PAG, and brain stem regions. Pain is an internal stressor that can compromise homeostasis and initiate patterns of physiological and behavioral response. When compromised, the function of the stress network is to restore homeostasis, affected by an increase in sympathetic outflow to improve cardiac output and divert blood flow to essential organs, coordinated with a decreased sensitivity to pain (12, 39). Sympathovagal balance and heart rate are initially maintained at baseline after SNI, possibly due to the activation of stress networks in the acute phase of injury. Following this early phase, there was a point of divergence at 7–10 days after SNI where the pain response either resolved back to normal function or was sustained over the postinjury period, perhaps signifying the transition from acute to chronic pain. Animals with sustained hyperalgesia behavior showed a significant decrease in heart rate and sympathovagal balance with an increase in vagal tone. A similar pattern of response consisting of a fall in heart rate and augmented HF power was also reported after chronic constriction injury of the sciatic nerve model of neuropathy (31). Human subjects have also been shown to respond with a decrease in sympathetic nerve activity and heart rate to sustained pain, although others demonstrate sympathoexcitation to the same stimulus, highlighting individual differences in autonomic responses to pain (19). The inability to maintain heart rate in the face of sustained pain behavior suggests that dysregulation in the stress circuitry could contribute to a chronic pain state. The lack of blood pressure increase in animals demonstrating persistent hyperalgesia might also reflect altered cardiovascular and pain interactions. However, it is consistent with the drop in heart rate seen in this study and with previous studies indicating that heart rate is more responsive to noxious stimulation than blood pressure (22, 53). On the other hand, blood pressure did not change despite the reduction in sympathovagal balance and heart rate. This apparent anomaly could be attributed to differential control of regional sympathetic outflows or adaptation as a consequence of enhanced circulating hormones such as angiotensin. Rat activity level was not monitored in this study. Although there were no clearly observed differences, it is possible that changes in heart rate could be associated with activity levels as a consequence of hyperalgesia behavior.

The sympathosensory responses to eSNL developed similarly to those in the SNI model described above, except that the Non-Hyperalgesia group demonstrated comparatively minimal pain behavior initially after injury, and the divergence between hyperalgesia and nonhyperalgesia behavior occurred earlier, at around 3 days. The earlier development of hyperalgesia could be attributed to the relatively more aggressive injury affecting both L4 and L5 spinal nerves that could include both femoral and sciatic input.

Neurons in the PAG are critical central components modulating sympathetic outflow and sensory afferent input. The PAG is subdivided into columns around the cerebral aqueduct based upon cell phenotype, connectivity, and function. The dorsal and dorsolateral columns of the PAG (dPAG) are associated with active strategies to avoid stressors, including sympathoexcitation and opioid-independent antinociception (32). In contrast, the ventrolateral PAG is associated with passive responses and recovery efforts including sympathoinhibition and opioid-dependent analgesia (32). Nociceptive inputs relayed from the superficial lamina of the spinal cord to the lateral and ventrolateral columns of the PAG

activate descending modulatory pathways that can inhibit or facilitate noxious afferent input in the dorsal horn (46). The organization of the neurocircuitry in the PAG that influences autonomic and pain responses is unknown. The same neurons may subservise both sympathetic and sensory functions, or coordination of activity of separate sympathetic and sensory neurons may occur. However, the dPAG produces increases in sympathetic nerve activity, blood pressure, heart rate, and analgesia, for which there is growing evidence for the involvement of the endocannabinoid system (6, 10, 11, 28, 39, 41, 59). The data presented here suggest that upregulation of FAAH leading to reduced anandamide in the dPAG contributes to the maladaptive pain responses and associated autonomic and cardiovascular disturbances in chronic neuropathic pain. Interestingly, the fMRI signal intensity in the dPAG, but not the ventral PAG, increases in human subjects that demonstrate reduced sympathetic activity in chronic pain, supporting dysregulation of this PAG region in pain states (35).

Although this study focused on the dPAG, endocannabinoid signaling in the vPAG may contribute to the autonomic adjustments evident in this study. CB1 receptors are distributed extensively throughout the dPAG and the vPAG in both somatodendritic and presynaptic structures (61). Neurons from both regions innervate the rostral region of the external nucleus ambiguus that contains cardiac parasympathetic preganglionic neurons with the dPAG projection mediating inhibitory and the vPAG mediating facilitatory effects (17, 30). The latter projection could contribute to the parasympathetic and bradycardic effects evident in the hyperalgesia rats.

Central antihyperalgesic actions of cannabinoid agonists have been demonstrated in a range of neuropathic pain models, and data from the present study suggest that the dPAG is a site of altered endocannabinoid signaling associated with pain relief (18, 34, 52). Anandamide content in the dPAG is lower in animals that developed persisting hyperalgesia and these data are supported by a positive correlation between transcript levels of mRNA for FAAH in the dPAG and hyperalgesia behavior. Also in accordance with these data, dPAG FAAH activity is increased in animals that demonstrate hyperalgesia responses at 21 days post-SNI. FAAH is a membrane protein expressed mainly in large outflow neurons and a primary regulator of brain anandamide concentrations by its hydrolysis to arachidonic acid and ethanolamide (8, 59). Interestingly, the contents of OEA and PEA, NAEs also catabolized by FAAH (26), trend to decrease but are not significantly altered in the hyperalgesic animals. We speculate that either anandamide synthesis is also decreased or a second enzyme involved in AEA degradation, for example, cyclooxygenase 2 (25), is also upregulated. FAAH activity in the dPAG of animals that do not maintain hyperalgesia responses 21 days after injury (mean  $2.25 \pm 0.47$  fmol ethanolamine formed/min/mg protein) is similar to baseline levels of dPAG FAAH activity (mean  $1.9 \pm 0.45$  fmol/ethanolamine formed/min/mg protein) (13). However, the mean FAAH activity level in the dPAG of animals that demonstrate hyperalgesia responses at 21 days post SNI is doubled at  $5.08 \pm 0.45$  fmol ethanolamine formed $\cdot$ min $^{-1}\cdot$ mg protein $^{-1}$ , suggesting that FAAH activity differences are a consequence of the nerve injury rather than a preexisting difference between the groups. Importantly, these data indicate that injury-induced upregulation of FAAH in the dPAG contributes to a maladaptive reduction of anandamide content that could contribute to the development of chronic pain after nerve injury. Animals that do not develop chronic

hyperalgesia maintain basal levels of FAAH. The origin of this heterogeneity of FAAH response to nerve injury is unknown.

In interpreting the experiments reported here, a possible mechanistic model to integrate our findings is shown in Fig. 7. Hyperalgesia and increased FAAH mRNA in the dPAG are also associated with attenuated sympathovagal balance and heart rate at 21 days postinjury, supporting a role for endocannabinoid signaling in facilitating the integrated stress response. Activated by pain, the normal function of the stress circuitry and enhanced endocannabinoid signaling would be to maintain sympathetic activity and attenuate pain responses to baseline as observed in animals that did not develop chronic pain behavior after injury. Dysfunction through upregulation of FAAH and reduced anandamide could contribute to decreased heart rate and increased sensitivity to pain.

### Perspectives and Significance

Our findings indicate that upregulated FAAH and reduced anandamide content in the dPAG are associated with hyperalgesia and reduced heart rate sustained weeks after nerve injury. These data provide support for continued evaluation of the use of FAAH inhibitors to address neuropathic pain management as explored for injury, inflammatory, noninflammatory, and chemotherapy-induced pain states (1, 9, 23, 34). These studies also demonstrate a need for additional studies in the regulation of FAAH expression, particularly following injury and chronic stress. The antinociceptive and autonomic effects of endocannabinoids in the dPAG are an example of the diverse functions of endocannabinoid signaling in various neural circuits and locations (26), encouraging future research into targeted therapy to address specific conditions and limit adverse side effects of systemic administration.

### ACKNOWLEDGMENTS

We thank V. Woyach for outstanding surgical and technical skills and C. Hermes, E. Koester, and R. Lange for excellent technical expertise.

#### GRANTS

This work was supported by Merit Review Award BX001863 from the U.S. Department of Veterans Affairs Biomedical Laboratory Research and Development Program (to Q. H. Hogan) and by the Research and Education Component of the Advancing a Healthier Wisconsin Endowment at the Medical College of Wisconsin (to C. J. Hillard).

### REFERENCES

1. Ahn K, Smith SE, Liimatta MB, Beidler D, Sadagopan N, Dudley DT, Young T, Wren P, Zhang Y, Swaney S, Van Becelaere K, Blankman JL, Nomura DK, Bhattachar SN, Stiff C, Nomanbhoy TK, Weerapana E, Johnson DS, Cravatt BF. Mechanistic and pharmacological characterization of PF-04457845: a highly potent and selective fatty acid amide hydrolase inhibitor that reduces inflammatory and noninflammatory pain. *J Pharmacol Exp Ther* 338: 114–124, 2011 10.1124/jpet.111.180257. [PubMed: 21505060]
2. Billman GE, Huikuri HV, Sacha J, Trimmel K. An introduction to heart rate variability: methodological considerations and clinical applications. *Front Physiol* 6: 55, 2015 10.3389/fphys.2015.00055. [PubMed: 25762937]

3. Blankman JL, Simon GM, Cravatt BF. A comprehensive profile of brain enzymes that hydrolyze the endocannabinoid 2-arachidonoylglycerol. *Chem Biol* 14: 1347–1356, 2007 10.1016/j.chembiol.2007.11.006. [PubMed: 18096503]
4. Bridges D, Ahmad K, Rice AS. The synthetic cannabinoid WIN55,212–2 attenuates hyperalgesia and allodynia in a rat model of neuropathic pain. *Br J Pharmacol* 133: 586–594, 2001 10.1038/sj.bjp.0704110. [PubMed: 11399676]
5. Bruehl S, Chung OY. Interactions between the cardiovascular and pain regulatory systems: an updated review of mechanisms and possible alterations in chronic pain. *Neurosci Biobehav Rev* 28: 395–414, 2004 10.1016/j.neubiorev.2004.06.004. [PubMed: 15341037]
6. Butler RK, Finn DP. Stress-induced analgesia. *Prog Neurobiol* 88: 184–202, 2009 10.1016/j.pneurobio.2009.04.003. [PubMed: 19393288]
7. Cannon JT, Prieto GJ, Lee A, Liebeskind JC. Evidence for opioid and non-opioid forms of stimulation-produced analgesia in the rat. *Brain Res* 243: 315–321, 1982 10.1016/0006-8993(82)90255-4. [PubMed: 7104742]
8. Cravatt BF, Giang DK, Mayfield SP, Boger DL, Lerner RA, Gilula NB. Molecular characterization of an enzyme that degrades neuromodulatory fatty-acid amides. *Nature* 384: 83–87, 1996 10.1038/384083a0. [PubMed: 8900284]
9. Cravatt BF, Lichtman AH. Fatty acid amide hydrolase: an emerging therapeutic target in the endocannabinoid system. *Curr Opin Chem Biol* 7: 469–475, 2003 10.1016/S1367-5931(03)00079-6. [PubMed: 12941421]
10. Dean C. Endocannabinoid modulation of sympathetic and cardiovascular responses to acute stress in the periaqueductal gray of the rat. *Am J Physiol Regul Integr Comp Physiol* 300: R771–R779, 2011 10.1152/ajpregu.00391.2010. [PubMed: 21228344]
11. Dean C. Cannabinoid and GABA modulation of sympathetic nerve activity and blood pressure in the dorsal periaqueductal gray of the rat. *Am J Physiol Regul Integr Comp Physiol* 301: R1765–R1772, 2011 10.1152/ajpregu.00398.2011. [PubMed: 21940402]
12. Dean C, Coote JH. Discharge patterns in postganglionic neurones to skeletal muscle and kidney during activation of the hypothalamic and midbrain defence areas in the cat. *Brain Res* 377: 271–278, 1986 10.1016/0006-8993(86)90868-1. [PubMed: 3730862]
13. Dean C, Hillard CJ, Seagard JL, Hopp FA, Hogan QH. Components of the cannabinoid system in the dorsal periaqueductal gray are related to resting heart rate. *Am J Physiol Regul Integr Comp Physiol* 311: R254–R262, 2016 10.1152/ajpregu.00154.2016. [PubMed: 27280429]
14. Djouhri L, Koutsikou S, Fang X, McMullan S, Lawson SN. Spontaneous pain, both neuropathic and inflammatory, is related to frequency of spontaneous firing in intact C-fiber nociceptors. *J Neurosci* 26: 1281–1292, 2006 10.1523/JNEUROSCI.3388-05.2006. [PubMed: 16436616]
15. Eckberg DL. Sympathovagal balance: a critical appraisal. *Circulation* 96: 3224–3232, 1997 10.1161/01.CIR.96.9.3224. [PubMed: 9386196]
16. Elmes SJ, Jhaveri MD, Smart D, Kendall DA, Chapman V. Cannabinoid CB2 receptor activation inhibits mechanically evoked responses of wide dynamic range dorsal horn neurons in naïve rats and in rat models of inflammatory and neuropathic pain. *Eur J Neurosci* 20: 2311–2320, 2004 10.1111/j.1460-9568.2004.03690.x. [PubMed: 15525273]
17. Farkas E, Jansen ASP, Loewy AD. Periaqueductal gray matter projection to vagal preganglionic neurons and the nucleus tractus solitarius. *Brain Res* 764: 257–261, 1997 10.1016/S0006-8993(97)00592-1. [PubMed: 9295220]
18. Farquhar-Smith WP, Egertová M, Bradbury EJ, McMahon SB, Rice AS, Elphick MR. Cannabinoid CB(1) receptor expression in rat spinal cord. *Mol Cell Neurosci* 15: 510–521, 2000 10.1006/mcne.2000.0844. [PubMed: 10860578]
19. Fazalbhoy A, Birznieks I, Macefield VG. Individual differences in the cardiovascular responses to tonic muscle pain: parallel increases or decreases in muscle sympathetic nerve activity, blood pressure and heart rate. *Exp Physiol* 97: 1084–1092, 2012 10.1113/expphysiol.2012.066191. [PubMed: 22581744]
20. Fox A, Kessingland A, Gentry C, McNair K, Patel S, Urban L, James I. The role of central and peripheral Cannabinoid1 receptors in the antihyperalgesic activity of cannabinoids in a model of neuropathic pain. *Pain* 92: 91–100, 2001 10.1016/S0304-3959(00)00474-7. [PubMed: 11323130]

21. Galiègue S, Mary S, Marchand J, Dussosoy D, Carrière D, Carayon P, Bouaboula M, Shire D, Le Fur G, Casellas P. Expression of central and peripheral cannabinoid receptors in human immune tissues and leukocyte subpopulations. *Eur J Biochem* 232: 54–61, 1995 10.1111/j.1432-1033.1995.tb20780.x. [PubMed: 7556170]
22. Gemes G, Rigaud M, Dean C, Hopp FA, Hogan QH, Seagard J. Baroreceptor reflex is suppressed in rats that develop hyperalgesia behavior after nerve injury. *Pain* 146: 293–300, 2009 10.1016/j.pain.2009.07.040. [PubMed: 19729245]
23. Guindon J, Hohmann AG. The endocannabinoid system and pain. *CNS Neurol Disord Drug Targets* 8: 403–421, 2009 10.2174/187152709789824660. [PubMed: 19839937]
24. Guindon J, Lai Y, Takacs SM, Bradshaw HB, Hohmann AG. Alterations in endocannabinoid tone following chemotherapy-induced peripheral neuropathy: effects of endocannabinoid deactivation inhibitors targeting fatty-acid amide hydrolase and monoacylglycerol lipase in comparison to reference analgesics following cisplatin treatment. *Pharmacol Res* 67: 94–109, 2013 10.1016/j.phrs.2012.10.013. [PubMed: 23127915]
25. Hermanson DJ, Hartley ND, Gamble-George J, Brown N, Shonesy BC, Kingsley PJ, Colbran RJ, Reese J, Marnett LJ, Patel S. Substrate-selective COX-2 inhibition decreases anxiety via endocannabinoid activation. *Nat Neurosci* 16: 1291–1298, 2013 10.1038/nn.3480. [PubMed: 23912944]
26. Hillard CJ. The endocannabinoids signaling system in the CNS: A primer. *Int Rev Neurobiol* 125: 1–47, 2015 10.1016/bs.irn.2015.10.001. [PubMed: 26638763]
27. Hogan Q, Sapunar D, Modric-Jednacak K, McCallum JB. Detection of neuropathic pain in a rat model of peripheral nerve injury. *Anesthesiology* 101: 476–487, 2004 10.1097/00000542-200408000-00030. [PubMed: 15277932]
28. Hohmann AG, Suplita RL, Bolton NM, Neely MH, Fegley D, Mangieri R, Krey JF, Walker JM, Holmes PV, Crystal JD, Duranti A, Tontini A, Mor M, Tarzia G, Piomelli D. An endocannabinoid mechanism for stress-induced analgesia. *Nature* 435: 1108–1112, 2005 10.1038/nature03658. [PubMed: 15973410]
29. Hohmann AG, Tsou K, Walker JM. Cannabinoid suppression of noxious heat-evoked activity in wide dynamic range neurons in the lumbar dorsal horn of the rat. *J Neurophysiol* 81: 575–583, 1999. [PubMed: 10036261]
30. Inui K, Murase S, Nosaka S. Facilitation of the arterial baroreflex by the ventrolateral part of the midbrain periaqueductal grey matter in rats. *J Physiol* 477: 89–101, 1994 10.1113/jphysiol.1994.sp020174. [PubMed: 8071891]
31. Jin Y, Sato J, Yamazaki M, Omura S, Funakubo M, Senoo S, Aoyama M, Mizumura K. Changes in cardiovascular parameters and plasma norepinephrine level in rats after chronic constriction injury on the sciatic nerve. *Pain* 135: 221–231, 2008 10.1016/j.pain.2007.05.020. [PubMed: 17611035]
32. Keay KA, Bandler R. Parallel circuits mediating distinct emotional coping reactions to different types of stress. *Neurosci Biobehav Rev* 25: 669–678, 2001 10.1016/S0149-7634(01)00049-5. [PubMed: 11801292]
33. Kelly S, Chapman V. Selective cannabinoid CB1 receptor activation inhibits spinal nociceptive transmission in vivo. *J Neurophysiol* 86: 3061–3064, 2001. [PubMed: 11731561]
34. Kinsey SG, Long JZ, O'Neal ST, Abdullah RA, Poklis JL, Boger DL, Cravatt BF, Lichtman AH. Blockade of endocannabinoid-degrading enzymes attenuates neuropathic pain. *J Pharmacol Exp Ther* 330: 902–910, 2009 10.1124/jpet.109.155465. [PubMed: 19502530]
35. Kobuch S, Fazalbhoy A, Brown R, Henderson LA, Macefield VG. Central circuitry responsible for the divergent sympathetic responses to tonic muscle pain in humans. *Hum Brain Mapp* 38: 869–881, 2017 10.1002/hbm.23424. [PubMed: 27696604]
36. Koutsikou S, Lawson SN. Increased reliability in a modified spinal nerve injury rat model of neuropathic pain, involving L5 transection plus L4 loose ligation. *J Physiol* 543: 113, 2002.
37. Lichtman AH, Cook SA, Martin BR. Investigation of brain sites mediating cannabinoid-induced antinociception in rats: evidence supporting periaqueductal gray involvement. *J Pharmacol Exp Ther* 276: 585–593, 1996. [PubMed: 8632325]

38. Lim G, Sung B, Ji RR, Mao J. Upregulation of spinal cannabinoid-1-receptors following nerve injury enhances the effects of Win 55,212-2 on neuropathic pain behaviors in rats. *Pain* 105: 275–283, 2003 10.1016/S0304-3959(03)00242-2. [PubMed: 14499445]
39. Lovick TA. Selective modulation of the cardiovascular response but not the antinociception evoked from the dorsal PAG, by 5-HT in the ventrolateral medulla. *Pflugers Arch* 416: 222–224, 1990 10.1007/BF00370249. [PubMed: 2352838]
40. Malliani A, Pagani M, Lombardi F, Cerutti S. Cardiovascular neural regulation explored in the frequency domain. *Circulation* 84: 482–492, 1991 10.1161/01.CIR.84.2.482. [PubMed: 1860193]
41. Martin WJ, Hohmann AG, Walker JM. Suppression of noxious stimulus-evoked activity in the ventral posterolateral nucleus of the thalamus by a cannabinoid agonist: correlation between electrophysiological and antinociceptive effects. *J Neurosci* 16: 6601–6611, 1996. [PubMed: 8815936]
42. Martin WJ, Patrick SL, Coffin PO, Tsou K, Walker JM. An examination of the central sites of action of cannabinoid-induced antinociception in the rat. *Life Sci* 56: 2103–2109, 1995 10.1016/0024-3205(95)00195-C. [PubMed: 7776838]
43. Martin WJ, Tsou K, Walker JM. Cannabinoid receptor-mediated inhibition of the rat tail-flick reflex after microinjection into the rostral ventromedial medulla. *Neurosci Lett* 242: 33–36, 1998 10.1016/S0304-3940(98)00044-5. [PubMed: 9509998]
44. Meng ID, Manning BH, Martin WJ, Fields HL. An analgesia circuit activated by cannabinoids. *Nature* 395: 381–383, 1998 10.1038/26481. [PubMed: 9759727]
45. Milicevi G. Low to high frequency ratio of heart rate variability spectra fails to describe sympatho-vagal balance in cardiac patients. *Coll Antropol* 29: 295–300, 2005. [PubMed: 16117339]
46. Millan MJ. Descending control of pain. *Prog Neurobiol* 66: 355–474, 2002 10.1016/S0301-0082(02)00009-6. [PubMed: 12034378]
47. Mitrirattanakul S, Ramakul N, Guerrero AV, Matsuka Y, Ono T, Iwase H, Mackie K, Faull KF, Spigelman I. Site-specific increases in peripheral cannabinoid receptors and their endogenous ligands in a model of neuropathic pain. *Pain* 126: 102–114, 2006 10.1016/j.pain.2006.06.016. [PubMed: 16844297]
48. Mogil JS. Pain genetics: past, present and future. *Trends Genet* 28: 258–266, 2012 10.1016/j.tig.2012.02.004. [PubMed: 22464640]
49. Nordin M, Fagius J. Effect of noxious stimulation on sympathetic vasoconstrictor outflow to human muscles. *J Physiol* 489: 885–894, 1995 10.1113/jphysiol.1995.sp021101. [PubMed: 8788952]
50. Patel S, Rademacher DJ, Hillard CJ. Differential regulation of the endocannabinoids anandamide and 2-arachidonylglycerol within the limbic forebrain by dopamine receptor activity. *J Pharmacol Exp Ther* 306: 880–888, 2003 10.1124/jpet.103.054270. [PubMed: 12808005]
51. Petrosino S, Palazzo E, de Novellis V, Bisogno T, Rossi F, Maione S, Di Marzo V. Changes in spinal and supraspinal endocannabinoid levels in neuropathic rats. *Neuropharmacology* 52: 415–422, 2007 10.1016/j.neuropharm.2006.08.011. [PubMed: 17011598]
52. Rahn EJ, Hohmann AG. Cannabinoids as pharmacotherapies for neuropathic pain: from the bench to the bedside. *Neurotherapeutics* 6: 713–737, 2009 10.1016/j.nurt.2009.08.002. [PubMed: 19789075]
53. Rigaud M, Gemes G, Abram SE, Dean C, Hopp FA, Stucky CL, Eastwood D, Tarima S, Seagard J, Hogan QH. Pain tests provoke modality-specific cardiovascular responses in awake, unrestrained rats. *Pain* 152: 274–284, 2011 10.1016/j.pain.2010.09.010. [PubMed: 20943317]
54. Rigaud M, Gemes G, Barabas ME, Chernoff DI, Abram SE, Stucky CL, Hogan QH. Species and strain differences in rodent sciatic nerve anatomy: implications for studies of neuropathic pain. *Pain* 136: 188–201, 2008 10.1016/j.pain.2008.01.016. [PubMed: 18316160]
55. Sheps DS, Bragdon EE, Gray TF III, Ballenger M, Usedom JE, Maixner W. Relation between systemic hypertension and pain perception. *Am J Cardiol* 70: 3F–5F, 1992 10.1016/0002-9149(92)90181-W.
56. Smith SB, Maixner DW, Greenspan JD, Dubner R, Fillingim RB, Ohrbach R, Knott C, Slade GD, Bair E, Gibson DG, Zaykin DV, Weir BS, Maixner W, Diatchenko L. Potential genetic risk factors



- for chronic TMD: genetic associations from the OPPERA case control study. *J Pain* 12, Suppl: T92–T101, 2011 10.1016/j.jpain.2011.08.005. [PubMed: 22074755]
57. Trevino C, Harl F, Deroon-Cassini T, Brasel K, Litwack K. Predictors of chronic pain in traumatically injured hospitalized adult patients. *J Trauma Nurs* 21: 50–56, 2014 10.1097/JTN.000000000000032. [PubMed: 24614292]
58. Tsou K, Nogueron MI, Muthian S, Sañudo-Pena MC, Hillard CJ, Deutsch DG, Walker JM. Fatty acid amide hydrolase is located preferentially in large neurons in the rat central nervous system as revealed by immunohistochemistry. *Neurosci Lett* 254: 137–140, 1998 10.1016/S0304-3940(98)00700-9. [PubMed: 10214976]
59. Walker JM, Huang SM, Strangman NM, Tsou K, Sañudo-Peña MC. Pain modulation by release of the endogenous cannabinoid anandamide. *Proc Natl Acad Sci USA* 96: 12198–12203, 1999 10.1073/pnas.96.21.12198. [PubMed: 10518599]
60. Walczak J-S, Pichette V, Leblond F, Desbiens K, Beaulieu P. Behavioral, pharmacological and molecular characterization of the saphenous nerve partial ligation: a new model of neuropathic pain. *Neuroscience* 132: 1093–1102, 2005 10.1016/j.neuroscience.2005.02.010. [PubMed: 15857713]
61. Wilson-Poe AR, Morgan MM, Aicher SA, Hegarty DM. Distribution of CB1 cannabinoid receptors and their relationship with mu-opioid receptors in the rat periaqueductal gray. *Neuroscience* 213: 191–200, 2012 10.1016/j.neuroscience.2012.03.038. [PubMed: 22521830]
62. Wu HE, Gemes G, Zoga V, Kawano T, Hogan QH. Learned avoidance from noxious mechanical stimulation but not threshold semmes weinstein filament stimulation after nerve injury in rats. *J Pain* 11: 280–286, 2010 10.1016/j.jpain.2009.07.011. [PubMed: 19945356]
63. Yaksh TL, Yeung JC, Rudy TA. Systematic examination in the rat of brain sites sensitive to the direct application of morphine: observation of differential effects within the periaqueductal gray. *Brain Res* 114: 83–103, 1976 10.1016/0006-8993(76)91009-X. [PubMed: 963546]

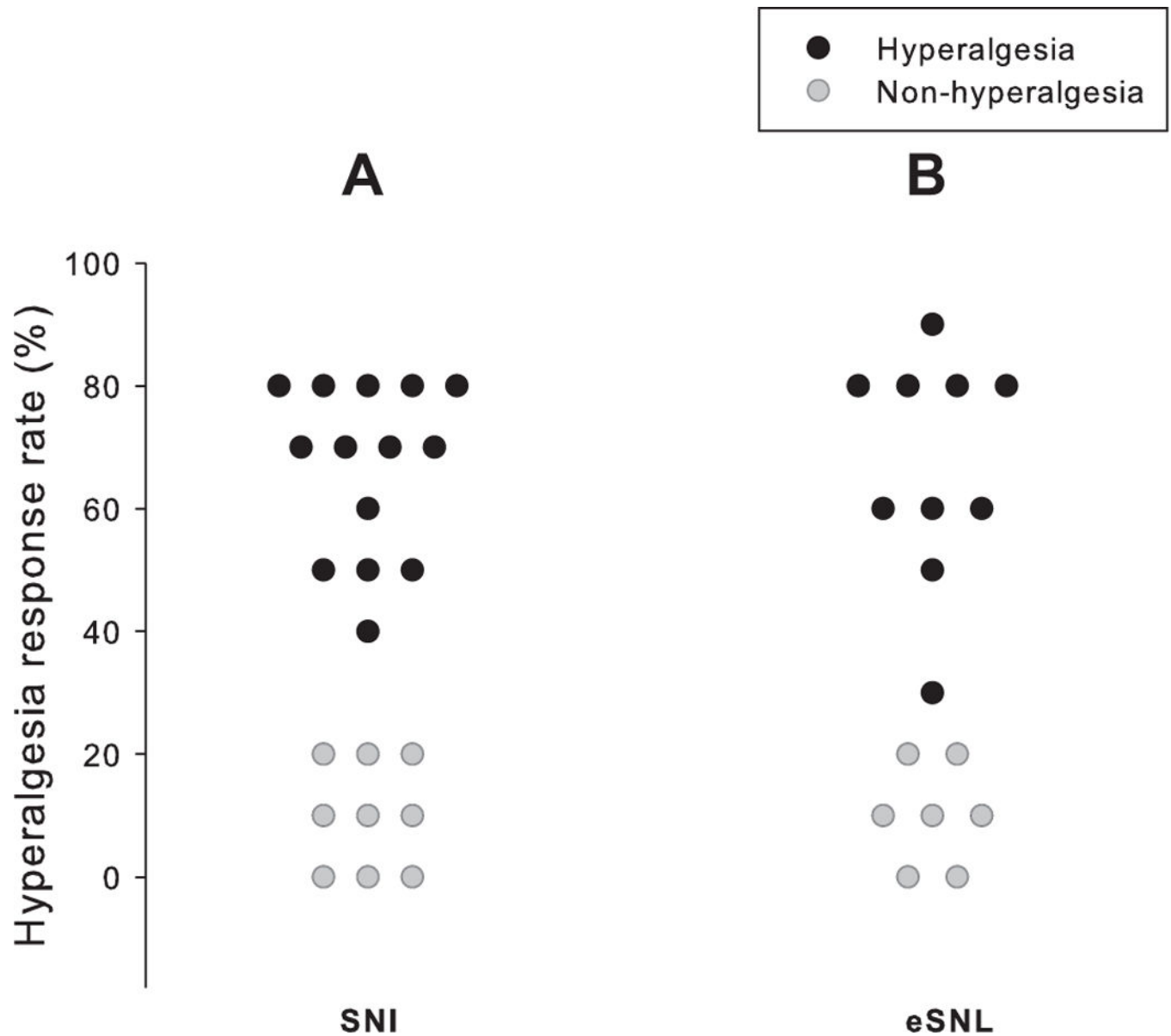


**Fig. 1.** Development of hyperalgesia responses to noxious hindpaw stimulation. At 21 days after injury, hyperalgesia response rates ranged from 0 to 80% after spared nerve injury (SNI, *A*) and 0 to 90% after enhanced spinal nerve ligation (eSNL, *B*). The Non-Hyperalgesia group demonstrated <20% response rate and the Hyperalgesia group >20%. Development of hyperalgesia behavior was similar for both paradigms with 14 of 23 SNI and 10 of 17 eSNL animals demonstrating hyperalgesia response rates > 20%.

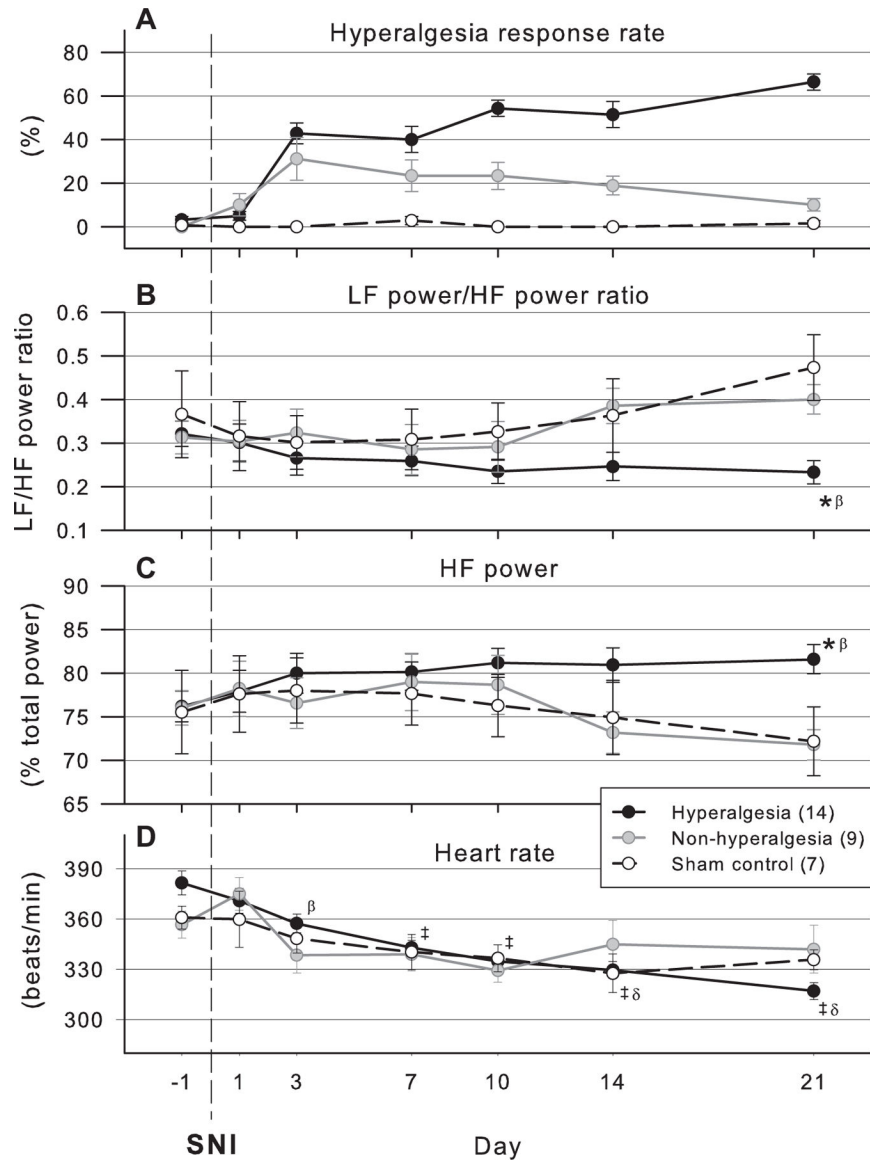


**Fig. 2.** Hyperalgesia response rate, heart rate variability and heart rate after spared nerve injury (SNI). *A*: hyperalgesia response rate. Animals were assigned according to hyperalgesia behavior on *day 21* after injury. The Hyperalgesia group ( $n = 14$ ) demonstrated  $>20\%$  hyperalgesia response rate and the Non-Hyperalgesia group  $<20\%$  hyperalgesia response rate ( $n = 9$ ). The Sham control group underwent surgery without nerve injury ( $n = 7$ ) and demonstrated no hyperalgesia type behavior. After an initial increase, the Non-Hyperalgesia group response resolved to Sham control levels in contrast to the Hyperalgesia group that maintained hyperalgesia behavior over the 21 days postinjury. *B*: low-frequency (LF) to high-frequency (HF) power ratio. Reflecting sympathovagal balance, the ratio of LF/HF power in the Hyperalgesia group decreased over time and was significantly lower than the Non-Hyperalgesia and Sham control groups ( $*F = 9.465$ ,  $P < 0.001$ ) and from baseline ( $P < 0.05$ ) at 21 days. *C*: HF power. Reflecting parasympathetic tone, the HF power in the

Hyperalgesia group increased over time and was significantly higher than the Non-Hyperalgesia and Sham control groups (\* $F=6.809$ ,  $P<0.005$ ) and from baseline ( $P<0.05$ ) at 21 days. *D*: heart rate. Heart rate showed no main effect of group at any time point but heart rate of the Hyperalgesia group decreased significantly over time postinjury. The Hyperalgesia group showed a significant decrease compared with baseline heart rate ( $F=16.594$ ) at *day 3* ( $\beta$ ,  $P<0.03$ ), and compared with baseline and *day 1* from all time points from *day 7* (denoted by ‡, *day 7*  $P<0.05$ ; *days 10–21*,  $P<0.001$ ). On *days 21* ( $P<0.001$ ) and *14* ( $P=0.01$ ) heart rate was also significantly decreased from *day 3*, denoted by  $\delta$ .

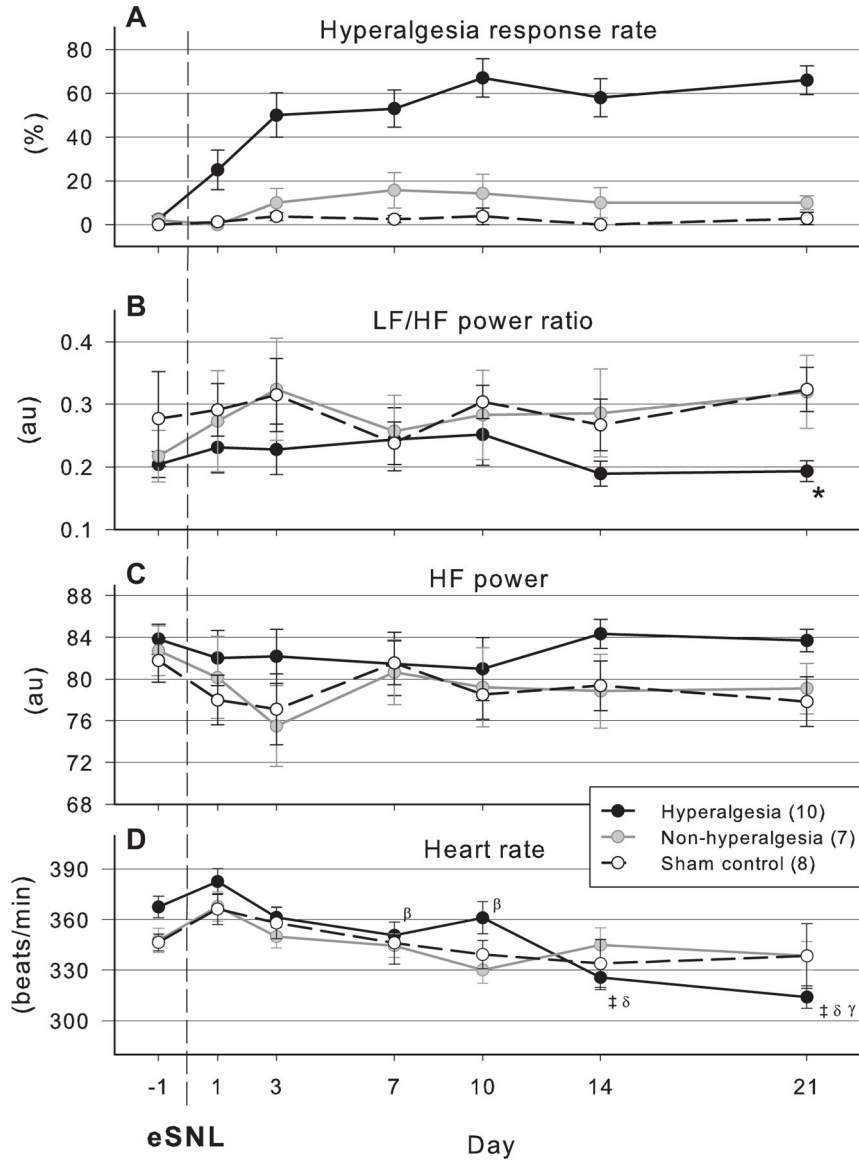


**Fig. 3.** Hyperalgesia response rate, heart rate variability, and heart rate after enhanced spinal nerve ligation (eSNL). *A*: hyperalgesia response rate. The Hyperalgesia group ( $n = 10$ ) demonstrated sustained hyperalgesia responses  $> 20\%$  over the 21 days postinjury whereas the Non-Hyperalgesia group ( $n = 7$ ) demonstrated  $< 20\%$  hyperalgesia response rates and Sham control ( $n = 8$ ) groups demonstrated no hyperalgesia behavior. *B*: LF/HF power ratio. Reflecting sympathovagal balance, the ratio of LF/HF power in the Hyperalgesia group on *day 21* was significantly lower than the Non-Hyperalgesia and Sham control groups ( $*F = 4.614, P < 0.05$ ). *C*: HF power. There was no difference in HF power between the three groups and no change from baseline over 21 days after eSNL, reflecting no change in vagal tone. *D*: heart rate. Heart rate showed no main effect of group at any time point but heart rate of the Hyperalgesia group decreased significantly over time postinjury. The Hyperalgesia group showed a significant decrease compared with baseline heart rate and *day 1* on *days 14*

and 21 ( $F=10.569$ ,  $\ddagger P<0.001$ ); compared with *day 1* ( $\beta$ , *day 10*,  $P=0.003$ ; *day 7*,  $P<0.05$ ); compared with *day 3* ( $\delta$ , *day 21*,  $P<0.001$ ; *day 14*  $P<0.02$ ); and compared with *day 7* ( $\gamma$ , *day 21*,  $P<0.02$ ).

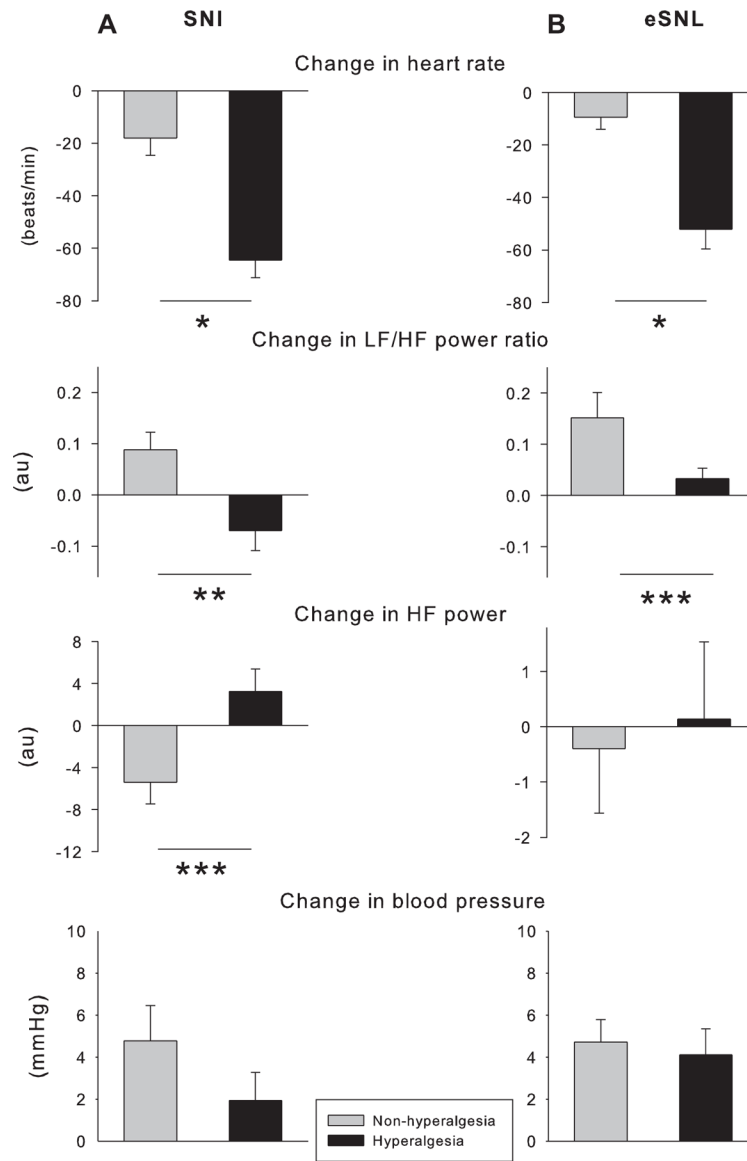


**Fig. 4.** Change in heart rate and heart rate variability after nerve injury. Graphs illustrate changes in HR, LF/HF power ratio, an indicator of sympathovagal balance and HF power, an indicator of parasympathetic tone at 21 days after SNI, and mean arterial blood pressure (A) and eSNL (B) in rats that demonstrated a hyperalgesia response rate to noxious stimulation of the hindpaw <20% (Non-Hyperalgesia; SNI  $n = 9$ , eSNL  $n = 7$ ) and >20% (Hyperalgesia; SNI  $n = 14$ , eSNL  $n = 10$ ). \* $P < 0.001$ ; \*\* $P = 0.002$ ; \*\*\* $P < 0.02$ .

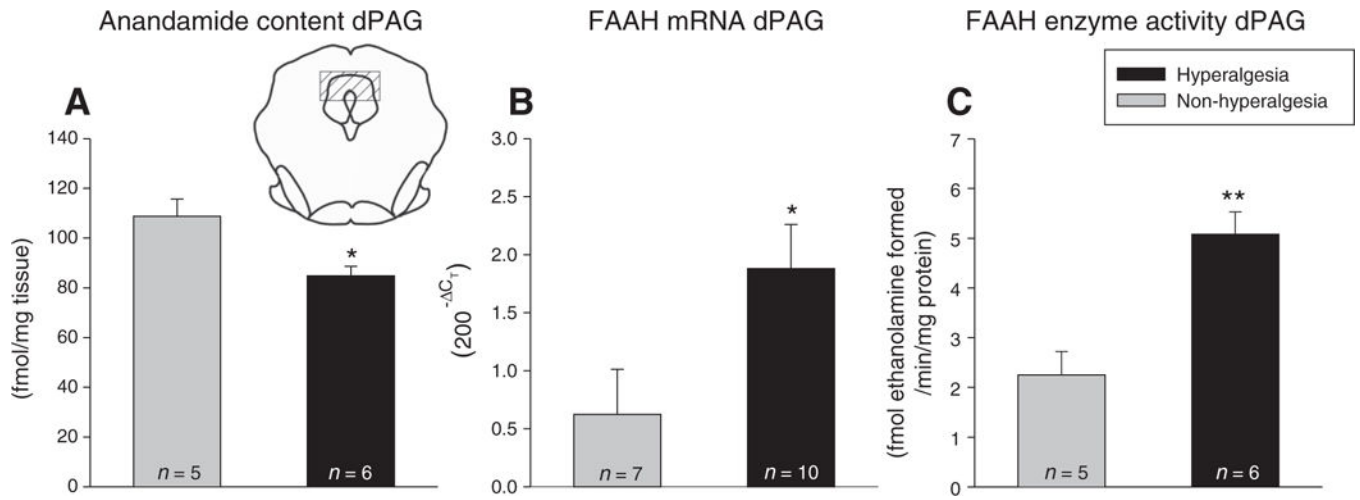


**Fig. 5.**

Anandamide content and enzyme activity in the dPAG after spared nerve injury. A diagrammatic representation of a section through the midbrain (*inset* in *A*) showing the shaded area that is excised for dPAG tissue analyses. Graphs illustrate decreased anandamide content (*A*), increased FAAH mRNA (*B*), and increased FAAH enzyme activity (*C*) in the dPAG of rats that developed >20% hyperalgesia responses (Hyperalgesia) compared with those that developed <20% hyperalgesia responses (Non-Hyperalgesia) at 21 days after spared nerve injury. \* $P < 0.02$ ; \*\* $P = 0.002$ ).



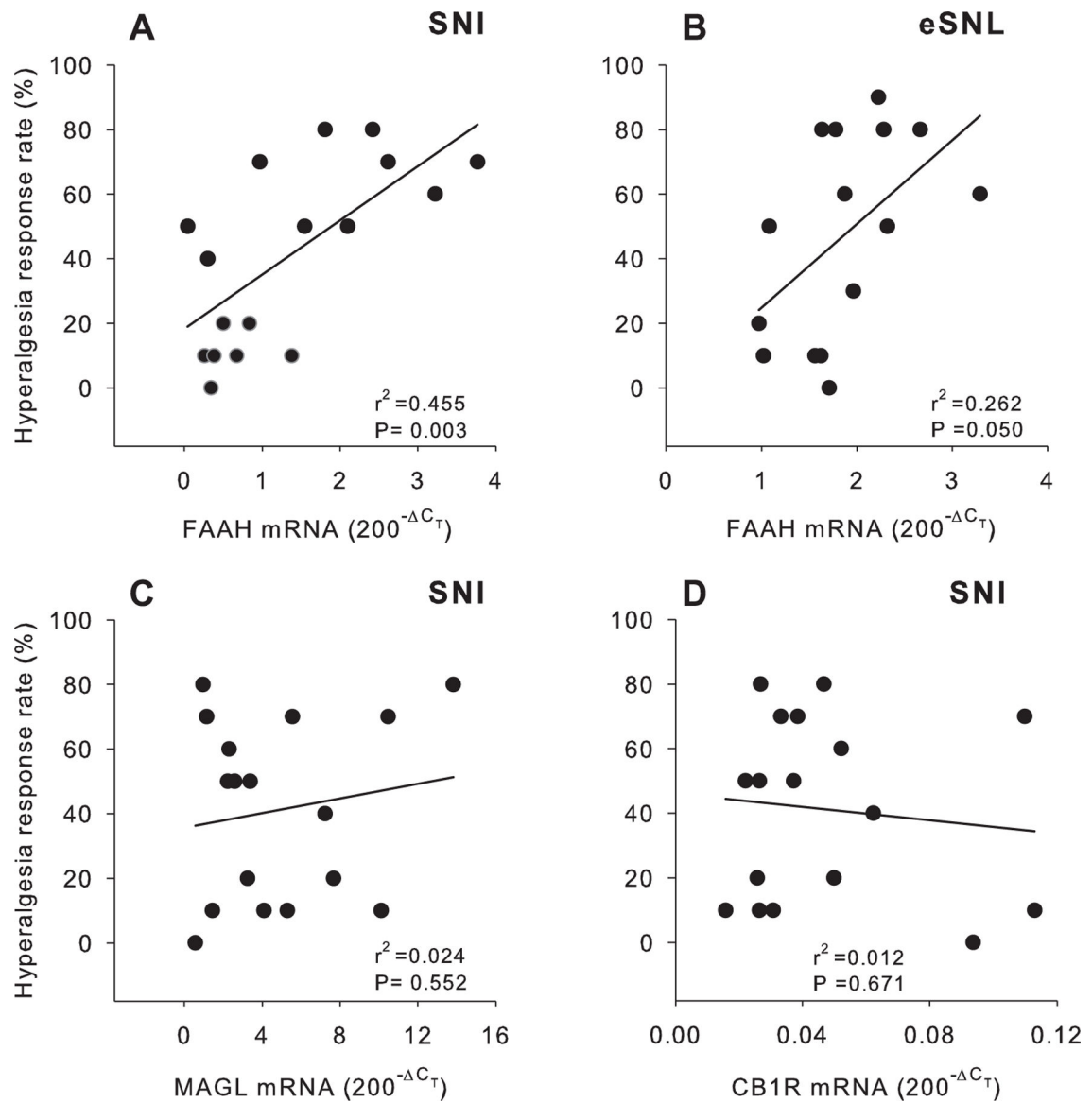


**Fig. 6.** Correlation between transcript levels of components of the endocannabinoid system and hyperalgesia responses. Linear regression analysis shows a significant inverse correlation between FAAH mRNA in the dPAG and hyperalgesia response rate at 21 days after SNI ( $n = 17$ ) (A) and eSNL ( $n = 15$ ) (B). There is no correlation between MAGL (C) or CB1 receptor mRNA (D) in the dPAG and hyperalgesia at 21 days after SNI.

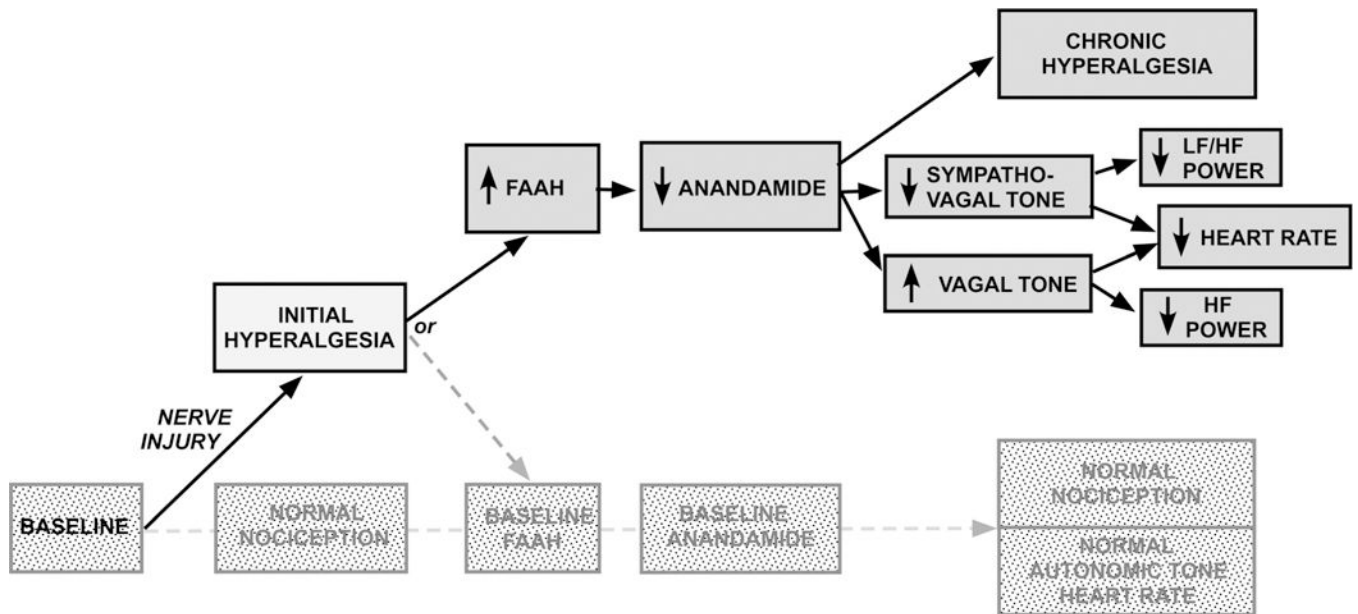


**Fig. 7.**

Model of development of chronic hyperalgesia after SNI. After an initial hyperalgesia response to nerve injury, animals that demonstrate an upregulation of FAAH and decreased anandamide content in the dPAG do not maintain sympathovagal balance or heart rate and develop chronic hyperalgesia. One-third of neuropathic animals demonstrate baseline levels of FAAH and anandamide in the dPAG and maintain cardiac autonomic tone and heart rate, and do not develop chronic hyperalgesia but resolve back to normal nociception.

**Table 1.**

Autonomic parameters are correlated to hyperalgesia and FAAH mRNA in the dPAG after nerve injury

	Vs. Hyperalgesia Response Rate		Vs. FAAH mRNA		
	$r^2$ value	<i>P</i> value	$r^2$ value	<i>P</i> value	
<i>Spared nerve injury</i>					
HR	-0.474	0.002*	HR	-0.144	0.133
LF/HF	-0.500	0.003*	LF/HF	-0.234	0.049*
HF	0.274	0.031*	HF	0.252	0.040*
<i>Enhanced spinal nerve ligation</i>					
HR	-0.462	0.004*	HR	-0.418	0.017*
LF/HF	-0.240	0.050*	LF/HF	-0.327	0.041*
HF	0.055	0.283	HF	0.168	0.163

Coefficient of determination ( $r^2$  value) and significance (*P* value) for hyperalgesia response rate and dorsal periaqueductal gray (dPAG) transcript levels of fatty acid amide hydrolase (FAAH) mRNA versus change in heart rate (HR), low frequency (LF)/high frequency (HF) power ratio indicator of sympathovagal balance, and HF power indicator of parasympathetic tone at 21 days after spared nerve injury ( $n = 17$ ) and enhanced spinal nerve ligation ( $n = 15$ )

\* Significance at  $P < 0.05$ .